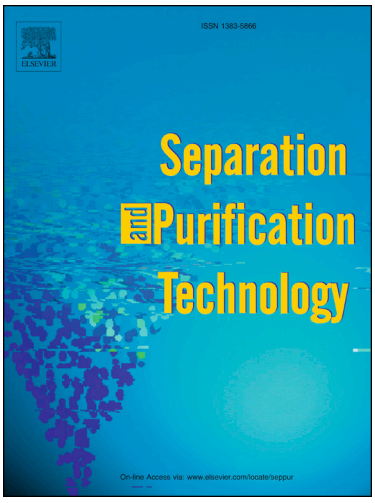

Parametric Optimisation for the Fabrication of Polyetherimide-sPEEK Asymmetric Membranes on a non-Woven Support Layer

Thomas J. Ainscough, Darren L. Oatley-Radcliffe, Andrew R. Barron

PII: S1383-5866(16)31576-3
DOI: http://dx.doi.org/10.1016/j.seppur.2017.05.045
Reference: SEPPUR 13758

To appear in: *Separation and Purification Technology*

Received Date: 31 August 2016
Revised Date: 25 May 2017
Accepted Date: 25 May 2017

Please cite this article as: T.J. Ainscough, D.L. Oatley-Radcliffe, A.R. Barron, Parametric Optimisation for the Fabrication of Polyetherimide-sPEEK Asymmetric Membranes on a non-Woven Support Layer, *Separation and Purification Technology* (2017), doi: http://dx.doi.org/10.1016/j.seppur.2017.05.045

Parametric Optimisation for the Fabrication of Polyetherimide-sPEEK Asymmetric Membranes on a non-Woven Support Layer

Thomas J. Ainscough[ab], Darren L. Oatley-Radcliffe*[ab], Andrew R. Barron[a]

[a] Energy Safety Research Institute (ESRI), Swansea University, Bay Campus, Fabian Way, Swansea SA1 8EN, UK

[b] Centre for Water Advanced Technologies and Environmental Research (CWATER), College of Engineering, Swansea University, Bay Campus, Fabian Way, Swansea SA1 8EN, UK.

*to whom correspondence should be addressed

Tel: + 44 (0)1792 606668

Email address: d.l.oatley@swansea.ac.uk

Abstract

Casting of a novel polyetherimide-sulfonated poly (ether ether ketone) membrane onto a non-woven support layer to improve mechanical strength and robustness of the resulting membrane is studied. The resultant membrane performance is optimised by considering the phase inversion parameters of polymer concentration, casting thickness, casting speed, evaporation time and coagulation bath temperature. Performance analysis was measured by membrane flux and rejection of PEG 10,000, along with structural characterisation of the membrane by SEM. Polymer concentration and coagulation bath temperature had the greatest influence on the final rejection properties of the membrane; increasing rejection from 0.72 to 0.96 when increasing from 16 wt% to 28 wt% and decreasing rejection from 0.95 to 0.60 when increasing the temperature from 3°C to 50°C respectively. Increasing the polymer concentration had the adverse effect of significantly reducing the permeation rate of the membrane from 50 LMH/bar to 1 LMH/bar when increasing from 16 wt% to 28 wt%. Using defined control of the phase inversion parameters the membrane was changed from an open pore ultrafiltration membrane with a molecular weight cut-off of >10 kDa to a much narrower pore size membrane in the nanofiltration range with a molecular weight

cut-off of ~3000 Da. The fabrication process for the optimised membrane is far more robust than the original process and is suitable for membrane mass production.

Keywords: *Phase inversion, Polyetherimide, Sulfonated Poly (Ether Ether Ketone), Membrane fabrication, Characterisation.*

1. Introduction

Membranes for the separation and concentration of valuable compounds have received significant attention in recent years and that interest shows no signs of slowing in the future [1]. This impetus is due to advancements in membrane technology, increasing cost of raw materials resulting in raw material or product previously wasted now recovered and recycled, and more stringent environmental legislation and regulation [2]. The attributing factors for the rise in popularity of membrane technologies when compared to their rivals are: simplicity, ease of large scale operation, low maintenance costs and relatively low energy requirements with no phase change and excellent selectivity. Ultrafiltration (UF) and nanofiltration (NF) are pressure driven membrane separation techniques situated between microfiltration (MF) and reverse osmosis (RO). These membranes are typically polymeric, asymmetric and consist of a low resistance support layer with a dense porous top layer also referred to as the active layer [3]. The nominal molecular weight cut-off (MWCO) of an NF membrane is typically in the range 150-2000 Da, this would suggest when assuming perfect cylindrical pores that the NF membrane active layer has an approximate pore size of 0.3 to 1 nm with UF membranes having larger pores [4]. The separation mechanisms of UF and NF are predominately related to steric and Donnan effects, with NF membranes having additional charge mechanisms such as dielectric exclusion due to the small pore size [5]. Thus, accurate control of the active layer to produce a given pore size distribution and surface chemistry is essential for successful separation performance.

Polyetherimide (PEI) is an ideal polymer for membrane fabrication as a result of improved chemical and thermal stability. PEI has been used extensively to fabricate both UF [6–8] and NF asymmetric membranes [9–11]. PEI membranes can be fabricated using the main manufacturing methods of spinning to produce hollow fibres [8] and casting to produce flat sheet membranes [9]. PEI membranes have found use in various applications including gas separation [12], pervaporation [6], solvent separation [13] and heavy metal recovery [14].

UF and NF are well-recognised separation technologies in the aqueous environment and research to improve the separation performance and anti-fouling properties of these membranes has been extensive [15]. The use of polymer blends and polymer solution additives have been developed to significantly increase the selectivity and chemical resistance of these membranes [16], especially within the field of fuel cells [17,18]. In particular polyether ether ketone (PEEK) and sulfonated polyether ether ketone (sPEEK) have been successfully used as co-polymers to improve permeability, rejection and fouling performance by improving the hydrophilicity of the resultant membrane [19,20].

Asymmetric membranes are typically prepared by the phase inversion and more specifically the immersion precipitation process. A casting solution containing the polymer is dissolved in a solvent, cast onto a flat surface and then immersed into an appropriate non-solvent coagulation bath. The membrane is formed or precipitated by the exchange of solvent and non-solvent due to the diffusion mechanism. The properties of a membrane fabricated via this method are dependent on the polymer casting conditions; most notably the polymer concentration and coagulation bath conditions. The influence of the phase inversion parameters has been studied previously for many polymers including polyvinylidene fluoride (PVDF) [21], polysulfone (PSF) [22,23] and lab synthesised PEEK based polymers [24].

This research is partially based on previous work producing a negatively charged UF and positively charged NF membrane by the phase inversion method, A6DT and PA6DT-C respectively [11,25,26]. This original methodology produced high performance membranes, however, following extensive testing, the membranes were found to be quite inflexible with a low tear resistance. In this study, a non-woven backing material is incorporated to improve the membrane mechanical strength and durability. The inclusion of the backing material has the potential to affect the physical properties of the resultant membrane due to the nature of the phase inversion method. As a result, the rejection and flux characteristics of the original A6DT membrane are no longer guaranteed for this new reinforced membrane, denoted A6DTR. Therefore, a phase inversion parameter study for the new membrane is conducted in order to optimise the membrane fabrication process and replicate the separation performance and excellent flux characteristics of the original membrane with the non-woven support added.

2. Experimental

2.1. Materials

All the membranes used in this study were prepared in the laboratory. PEI, 1-methyl-2-pyrrolidinone (NMP), 1,4-Dioxane and tetrahydrofuran (THF) were purchased in high purity form from Sigma-Aldrich (UK). Fumion E sPEEK was purchased from FuMA-Tech (Germany) and has an ion exchange capacity of 1.95 mmol/g. The chemical structures of PEI and sPEEK are shown in Fig. 1. PEI and sPEEK were dried at 100 °C for at least 24 h prior to use, all solvents were used as received. Ultra-pure water (DI) for the coagulation bath and characterisation was obtained from a Millipore ELIX 5 unit (Millipore UK Ltd., UK). The uncharged solute used to characterise the produced membranes was Poly Ethylene Glycol (PEG) with an average molecular weight of 10,000 (Fisher Scientific, UK) and was used as received.

2.2. Membrane Preparation

Asymmetric membranes were composed of predetermined quantities of polymer and solvent; compositions are provided in Table 1. Firstly, PEI was dissolved in NMP at a temperature of approximately 60 °C with magnetic stirring at 300 rpm to ensure the complete dissolution of the polymer. Then additives of SPEEK, THF and 1,4-dioxane were dissolved in the prepared PEI–NMP solutions with magnetic stirring at 200 rpm at room temperature for at least 4 h. The casting solutions were maintained at room temperature with no stirring for at least 1 day to release trapped air bubbles. The solutions were then covered using Parafilm (Fisher Scientific, UK) throughout the preparation stage to prevent contact with air and moisture. The polymer solution was then cast as a viscous film on a Polyester (PET) non-woven fabric CraneMat CU632 (Neenah Technical Materials, USA). Casting was conducted using a RK Print K101 bench casting machine (RK Print, UK).

The phase inversion parameters studied were: casting thickness, casting speed, evaporation time and coagulation bath temperature. The parameters outside of control due to the nature of the laboratory environment were air temperature and air humidity. These uncontrolled parameters can affect the membrane fabrication process and were recorded at the time of fabrication and included in the reported data. Unless otherwise stated, the membrane casting conditions were as follows:

- Casting thickness, 400 µm.
- Cast speed, 5.8 cm/s.
- Evaporation time, 30 s.
- Coagulation bath temperature, 20 °C

The casting films were immersed in deionised water (DI) and maintained at room temperature for 2 h. The membranes were then moved to fresh DI water for 1 day. Following solvent exchange, the prepared membranes were stored in fresh DI water until characterisation. Table 1 includes the typical composition for the membrane fabrication experiments including the polymer concentration experiments which adjusted the ratio of total polymer to total solvent using 22 wt% as the normalised value.

2.3. Membrane characterisation

2.3.1. Scanning electron microscopy

Scanning electron microscopy of membranes is a widely used technique capable of producing high resolution images of near atomic scale dimensions that are highly useful for the structural characterisation of membranes [32]. SEM was performed using a Hitachi S4800 Scanning Electron Microscope (Hitachi, USA). The membrane samples were dried using a vacuum desiccator and coated with 5nm of chromium using a Quorum sputter coater Q150R-ES (Quorum Technologies, UK) prior to observation to reduce sample charging.

2.3.2. Filtration Experiments

2.3.2.1. Experimental Setup

The membranes were tested for their filtration performance and rejection characteristics. Membrane performance was characterised by pure water membrane flux and rejection of a non-charged solute (PEG 10,000). All experiments were conducted at room temperature (22 ± 1 °C) and pH 6.0 ± 0.2, which is the pH of the DI water used throughout the study. The filtration studies were carried out using a commercially available stirred frontal filtration system (Membranology HP350 Filtration Cell, Membranology Ltd., UK), previously described by Oatley-Radcliffe et al. [27] and illustrated in Fig. 2. The cell has an operating capacity of 350 ml feed solution and an effective membrane surface area of 41.8 cm^2. The

filtration solutions were stirred magnetically at 300 rpm, previously shown to be the maximum practical stirrer speed [27]. Each membrane was initially subjected to pure water pressurisation at a pressure of 5 bar(g) until a stable flux was evident. Following pressurisation, membrane flux was recorded for each membrane between 1 bar and 5 bar in 1 bar increments. Subsequently, the solute rejection was measured using PEG 10,000 all at a concentration of 0.5 g/l with a constant applied pressure of 2 bar(g). At 28 wt% the membranes permeance is greatly limited, therefore to achieve a suitable result within an efficient timescale the membrane performance was evaluated at 5, 10, 15, 20 and 25 bar(g) and using this data extrapolated to 1 to 5 bar for comparison purposes. Also, due to the low permeance rate at 28 wt%, the rejection data was evaluated with an applied pressure of 20 bar(g) instead of the usual 2 bar(g). The concentration of PEG for the feed solution and permeate samples was analysed using a total organic carbon analyser (Shimadzu TOC-LCPH, Shimadzu Corporation UK). Rejection measurements were based on 20 ml of permeate once the initial 5 ml of permeate was discarded, 25 ml removed in total. After each rejection experiment the membrane was rinsed with DI water to remove any residual solute.

2.3.2.2. Rejection Theory

The experimental rejection characteristics of a membrane are usually defined by the observed rejection:

$$R_{obs} = 1 - \frac{C_P}{C_F} \quad (1)$$

where C_F and C_P are the concentrations of the feed and permeate respectively. However, due to concentration polarisation the concentration at the membrane surface, C_W is higher than that of the bulk feed concentration, C_F. Therefore, real rejection of the solute, R_{real}, which is always equal to or greater than R_{obs} is defined as:

$$R_{real} = 1 - \frac{C_P}{C_W} \quad (2)$$

The concentration at the wall, C_W, can be calculated indirectly using a suitable model for concentration polarisation [28]. The approach to concentration polarisation taken in this

study is that of the infinite rejection method first reported by Nakao and Kimura [29] and given as:

$$\exp\left(\frac{J_v}{k}\right) = \frac{C_W - C_P}{C_F - C_P} \quad (3)$$

where k is the mass transfer, defined as:

$$k = \frac{D_{eff,\infty}}{\delta} \quad (4)$$

and $D_{eff,\infty}$ is the diffusion coefficient at infinite dilution and δ is the thickness of the concentration polarisation layer.

The mass transfer coefficient may be determined experimentally by the substitution of equation (a) and (b) into equation (c), yielding:

$$\ln\left(\frac{1-R_{obs}}{R_{obs}}\right) = \frac{J_v}{k} + \ln\left(\frac{1-R_{real}}{R_{real}}\right) \quad (5)$$

In this case, the mass transfer coefficient may be represented as

$$k = a\omega^n \quad (6)$$

where a and n are predetermined constants and ω is the stirrer speed. For the Membranology cell these constants are 2.993 x 10^{-6} and 0.415 respectively [27].

3. Results and Discussion

3.1. The effect of polymer concentration on membrane performance

Polymer solutions containing concentrations between 16 wt% and 28 wt% were cast in 3% increments with a wet thickness of 400 µm. Previous studies suggest that as the polymer concentration increases the membrane properties will move from an ultrafilter towards a nanofilter, with an increase in solute rejection but also a reduction in permeance [10]. Fig. 3

illustrates the membrane performance characteristics for the resultant polymer blends. The effect of polymer concentration on the A6DTR membrane performance agrees with the aforementioned literature, demonstrating a linear reduction in membrane flux as the polymer concentration is increased, 50 LMH/bar to 1 LMH/bar over the range studied. The rejection of the non-charged solute does not follow the trend expected from literature results with the solute real rejection reducing slightly from 0.72 to 0.69 for 16 wt% and 19 wt% respectively, then notably dropping to 0.36 at 22 wt%. The membrane selectivity then increases significantly to 0.93 and 0.96 at 25 wt% to 28 wt% respectively, which is typicaly expected behaviour. The reduced flux and increased solute rejection at the higher concentration range is a result of a thicker, denser sponge like active layer with reduced macrovoid finger like structure support as shown in the SEM images of Fig. 4. Most notably between Fig. 4(a) and Fig. 4(e), 16 wt% and 28 wt% respectively. 16 wt% shows a thin active layer with very large macrovoids beneath the finger-like pores, whereas at 28 wt% a considerably thicker active layer has formed with a tight void-less structure support. The 22 wt% data will be discussed further in the next section.

3.2. The effect of casting thickness on membrane performance

The polymer solution was cast with a wet thickness between 100 µm and 500 µm in 100 µm increments. The membrane morphology has a distinct change between 100 µm and 500 µm as shown by the SEM cross section images in Fig. 5. During phase inversion the liquid polymer film thickness always shrinks considerably as a result of the solvent being diffused during coagulation reducing the overall solution volume. The SEM cross sections were measured and the films shrank by 74 % for the 100 µm to 400 µm thickness membranes and 62 % for the 500 µm, the difference can be accounted for by the production of large macrovoids in the polymer substructure.

At 100 µm, the SEM image Fig. 5(a) shows no discernible active layer, this also agrees with the recorded flux measurements, a specific flux of 316 LMH/bar. The flux is considerably higher than would be expected for a membrane of UF/NF type. The rejection of PEG 10,000 for this membrane was 0%. As a result of the high flux, PEG 10000 rejection and features of the cross section SEM image, the polymer is assumed to have mostly absorbed into the large open pores of the non-woven backing layer and no distinct active layer or substructure formation was observed.

At 200 µm a sponge like active layer with finger like voids in the substructure begins to form. These finger like voids increase in quantity and length as the casting film thickness is further increased to 500 µm, see Fig. 5(b) to (e). The membrane performance for the cast thicknesses from 200 to 500 µm is shown in Fig. 6 and shows a clear decrease in flux from 93 LMH/bar to 46.5 LMH/bar across the range. This result can be accounted for by an increase in hydraulic resistance of the membrane as the pore size decreases, despite the fact the active layer thickness remains constant; a phenomena observed in previous studies [8-11]. Also, the substructure will offer some additional resistance which will increase with the length of the void formed. Rejection increases linearly from 0.93 to 0.97 for 200 µm to 500 µm cast thickness respectively. The increase in rejection agrees with the flux reduction in that the pores of the active layer are becoming smaller at the larger cast thicknesses. From this rejection data an observation can be made that the 22 wt% polymer concentration experiment in section 3.1 was an anomaly, the data does not concur with the thickness variation experiments in this section which were all cast with 22 wt% polymer solutions and had a rejection that was greater than 0.93 between 200 µm and 500 µm. The only available explanation for this anomaly is either a membrane defect or a change in the laboratory environmental conditions. In the event of a membrane defect an increase in the permeate flowrate would be expected. However, as this wasn't the case the only be deduction to be made must be that the uncontrollable laboratory conditions of temperature and humidity must have affected the membrane. Upon further scrutiny of the environmental conditions, the thickness experiments were conducted at an air temperature of 19 °C ±1 °C and relative humidity of 39 % ±1 %. Whereas, the polymer concentration experiments were conducted at an air temperature of 23 °C ±2 °C and relative humidity of 50 % ±2 %. This may explain the behaviour observed.

3.3. The effect of casting speed on membrane performance

The effect of shear rate has been previously reported to show an adverse effect on the resultant membrane performance when the polymer is cast [30,31]. Therefore, the effect of shear rate by varying the casting speed at a constant thickness was investigated to discover if the PEI-sPEEK blend membranes are affected. The actual casting speeds used were 1.8 cm/s, 3.3 cm/s, 5.7 cm/s, 8.3 cm/s and 11.1 cm/s. Fig. 7 shows flux data with an optimal curve reaching a maximum between 5.7 cm/s and 8.3 cm/s equivalent to a shear rate of 145

s^{-1} and 209 s^{-1} respectively. The rejection characteristics of the membrane do not demonstrate an optimum, but decrease linearly from 0.98 to 0.92 for the same casting conditions. The membrane cross-sections, shown in Fig. 8, were examined to determine the nature of these characteristics. The SEM images all show a dense sponge like active layer with finger like sub structure. The top active layer shows very little variance which would explain the lack of major variation in the rejection experiments. However, the optimum flux membranes (Fig. 8 c and d) show a wider finger like sub structure and some macrovoids, whilst at the higher and lower casting speeds the images show a thinner finger structure and the macrovoids are replaced with another dense layer beneath the finger like sub structure. This additional dense sub layer explains the low permeance rates experienced away from the optimum. These results would suggest that the membrane is indeed affected by the shear rate of the cast, however, the magnitude in variation of both the resulting flux and rejection behaviour of the produced membranes suggests that casting speed has only minor influence on the fabrication process.

3.4. The effect of evaporation time on membrane performance

To study the influence of the evaporation time prior to immersion in the coagulation bath, a standard polymer solution was allowed to evaporate for a set time of either 10 s, 20 s, 30 s, 45 s, 60 s or 90 s. As shown in Fig. 9, increasing the evaporation time significantly decreases the flux and also decreases the solute retention. The permeance drops drastically beyond 20 s of evaporation time from 38.1 LMH/bar to reach a plateau at 60 s to 90s of 18 LMH/bar. The drop in flux can once again be explained due to the membrane morphology; a longer evaporation time results in a thicker more dense active layer along with a greatly diminished finger like sub structure, as shown in Fig. 10. Phase inversion theory predicts this outcome: as more solvent evaporates over an extended evaporation time, a localised increase in polymer concentration occurs, slowing down diffusion during coagulation. As a result, a membrane with few to no macrovoids is formed. The slight drop in rejection is a more difficult phenomenon to explain, this would suggest that with additional time the active layer pores begin to form and then develop into a larger overall pore size distribution. Evaporation time as a phase inversion parameter is a particularly difficult constraint to examine in an open laboratory environment due to the fact the parameter is at best

pseudo-controlled and should not be considered a suitable variable for tuning a membrane unless the laboratory environment is fully controlled.

3.4. The effect of coagulation bath temperature on membrane performance

The final parameter investigated in this study was the coagulation bath temperature. The DI water used in the coagulation bath was heated using a hotplate or chilled by using frozen di water cubes made prior to use depending on the temperature required. The temperature range studied was 3 °C to 50 °C. By comparison to the other phase inversion parameters investigated, the results of the bath temperature variation provided the most unexpected trends. At the lower end of the range between 3 °C and 20 °C the flux performance of the membrane improves slightly from 37 LMH/bar to 40.5 LMH/bar as the temperature is increased, with only a slight deterioration in rejection performance from 0.95 to 0.93 as shown in Fig. 11. The SEM cross sections, Fig. 12, for these membranes show a polymer thickness increase. Whilst the active layer thickness does not vary greatly the finger substructure lengthens substantially as the temperature increases. The substructure reaches a maximum length at 30 °C at which point the flux reaches a minimum and the rejection performance begins to decline. At 40 °C the substructure appears to shrink, however, macrovoids are now present beneath the substructure for the first time to account for this contraction and an improvement in permeance is noted. At 50 °C the membrane experiences a drastic improvement in the flux but the rejection approaches the lowest value of 0.60. The increase in membrane permeance from 23 LMH/bar at 40 °C to 41 LMH/bar at 50 °C resulted in further membranes being cast to verify this surprising data point, and the result was confirmed. Macrovoids are once again present at 50 °C, therefore along with the poor rejection data, an assumption can be made that at high temperature, >40 °C, the solvent is more readily diffused into the hot water and large pores are formed in the active layer. Overall, this data suggests the optimum bath temperature for stable membrane properties is <20 °C.

4. Conclusions

The parameters of the phase inversion fabrication method for preparing PEI/sPEEK blend asymmetric membranes on a non-woven support were successfully investigated. Increasing

the polymer concentration of the casting solution from 16 wt% to 28 wt % had the outcome of improving retention from 72% to 96% but significantly lowered the permeance. Casting thickness had little effect on the rejection of the uncharged solute increasing only 4% between 200 µm and 500µm. However, an increased casting thickness caused a significant drop in flux performance, 46 LMH/bar, despite the formation of macrovoids. Membrane rejection was not greatly influenced by the casting speed for the polymer solution, with only a 6% drop in rejection with an increased cast speed. The optimum flux performance, 55.45 LMH/bar, was found within the middle of the experimented range 5.7 cm/s to 8.3 cm/s. Evaporation time was a parameter deemed unreliable as a pseudo-controlled variable, but was determined to be a suitable parameter for densification of the active layer. The additional energy requirements to cool the coagulation bath temperature from ambient room temperature (20°C) would prove inefficient for the minor performance benefits gained but would severe to improve the reliability and robustness of the resulting membranes.

This study found the optimum casting parameters for a PEI/sPEEK blend membrane to create a high flux UF membrane with MWCO >10 kDa are: polymer concentration of 16 wt%, casting thickness of 200 µm, casting speed of 7 cm/s, evaporation time of 10 s and coagulation bath temperature of 50 °C. The study also determined for a high rejection UF/NF membrane with MWCO ~ 3kDa, the optimum casting parameters for a PEI/sPEEK blend membrane are: polymer concentration of 28 wt%, casting thickness of 500 µm, casting speed of 2 cm/s, evaporation time of 10 s and coagulation bath temperature of 20 °C. Depending on the application a compromise between the two extremes may be desirable and tuning of the membrane properties is demonstrated.

In this study, the initial A6DT membrane was successfully cast onto a non-woven support layer in order to improve mechanical strength and durability. By varying the phase inversion parameters the resulting A6DTR membrane was tuned from an open pore ultrafiltration membrane to a more narrow pore nanofiltration type membrane. Future work is now required in order to cast this optimised membrane in large flat sheet format and form the resultant membrane into a spiral wound module suitable for industrial applications.

Acknowledgements

Financial support to T.J. Ainscough was provided by the Robert A. Welch Foundation and the Welsh government Ser Cymru programme.

References

[1] Membranes Market by Type (Polymeric membranes, Ceramic membranes, and others), by Technology (MF, RO, UF, Pervaporation, Gas Separation, Dialysis, NF, and Others), by Region (North America, Europe, Asia-Pacific, the Middle East & Africa, and Latin America), and by Application - Global Forecast to 2020. http://www.marketsandmarkets.com/Market-Reports/membranes-market-1176.html.

[2] S. Šostar-Turk, I. Petrinić, M. Simonič, Laundry wastewater treatment using coagulation and membrane filtration, Resour. Conserv. Recycl. 44 (2005) 185–196.

[3] N. Hilal, H. Al-Zoubi, N.A. Darwish, A.W. Mohammad, M. Abu Arabi, A comprehensive review of nanofiltration membranes:Treatment, pretreatment, modelling, and atomic force microscopy, Desalination. 170 (2004) 281–308.

[4] D.L. Oatley-Radcliffe, S.R. Williams, T.J. Ainscough, C. Lee, D.J. Johnson, P.M. Williams, Experimental determination of the hydrodynamic forces within nanofiltration membranes and evaluation of the current theoretical descriptions, Sep. Purif. Technol. 149 (2015) 339–348.

[5] D.L. Oatley, L. Llenas, N.H.M. Aljohani, P.M. Williams, X. Martínez-Lladó, M. Rovira, et al., Investigation of the dielectric properties of nanofiltration membranes, Desalination. 315 (2013) 100–106.

[6] X. Feng, R.Y.M. Huang, Preparation and performance of asymmetric polyetherimide membranes for isopropanol dehydration by pervaporation, J. Memb. Sci. 109 (1996) 165–172.

[7] M. Khayet, C.. Feng, T. Matsuura, Morphological study of fluorinated asymmetric polyetherimide ultrafiltration membranes by surface modifying macromolecules, J. Memb. Sci. 213 (2003) 159–180.

[8] L.-Q. Shen, Z.-K. Xu, Z.-M. Liu, Y.-Y. Xu, Ultrafiltration hollow fiber membranes of

sulfonated polyetherimide/polyetherimide blends: preparation, morphologies and anti-fouling properties, J. Memb. Sci. 218 (2003) 279–293.

[9] Kim, I-C, K-H. Lee and T-M. Moon, Preparation and characterization of integrally skinned uncharged polyetherimide asymmetric nanofiltration membrane, J. Memb. Sci. 183 (2001) 235–247.

[10] I.-C. Kim, H.-G. Yoon, K.-H. Lee, Formation of integrally skinned asymmetric polyetherimide nanofiltration membranes by phase inversion process, J. Appl. Polym. Sci. 84 (2002) 1300–1307.

[11] W.R. Bowen, S. Cheng, T. Doneva, D. Oatley, Manufacture and characterisation of polyetherimide/sulfonated poly(ether ether ketone) blend membranes, J. Memb. Sci. 250 (2005) 1–10.

[12] K. Kneifel, K.-V. Peinemann, Preparation of hollow fiber membranes from polyetherimide for gas separation, J. Memb. Sci. 65 (1992) 295–307.

[13] M. Namvar-Mahboub, M. Pakizeh, Development of a novel thin film composite membrane by interfacial polymerization on polyetherimide/modified SiO2 support for organic solvent nanofiltration, Sep. Purif. Technol. 119 (2013) 35–45.

[14] A. Nagendran, A. Vijayalakshmi, D.L. Arockiasamy, K.H. Shobana, D. Mohan, Toxic metal ion separation by cellulose acetate/sulfonated poly(ether imide) blend membranes: effect of polymer composition and additive., J. Hazard. Mater. 155 (2008) 477–85.

[15] D. Rana, T. Matsuura, Surface modifications for antifouling membranes., Chem. Rev. 110 (2010) 2448–71.

[16] D.R. Paul, POLYMER BLENDS, Volume 1, Elsevier, 2012.

[17] J. Kerres, A. Ullrich, F. Meier, T. Häring, Synthesis and characterization of novel acid–base polymer blends for application in membrane fuel cells, Solid State Ionics. 125 (1999) 243–249.

[18] K.D. Kreuer, On the development of proton conducting polymer membranes for hydrogen and methanol fuel cells, J. Memb. Sci. 185 (2001) 29–39.

[19] P. Xing, G.P. Robertson, M.D. Guiver, S.D. Mikhailenko, K. Wang, S. Kaliaguine,

Synthesis and characterization of sulfonated poly(ether ether ketone) for proton exchange membranes, J. Memb. Sci. 229 (2004) 95–106.

[20] W.R. Bowen, T.A. Doneva, H. Yin, The effect of sulfonated poly(ether ether ketone) additives on membrane formation and performance, Desalination. 145 (2002) 39–45.

[21] M.G. Buonomenna, P. Macchi, M. Davoli, E. Drioli, Poly(vinylidene fluoride) membranes by phase inversion: the role the casting and coagulation conditions play in their morphology, crystalline structure and properties, Eur. Polym. J. 43 (2007) 1557–1572.

[22] A. Ismail, P. Lai, Effects of phase inversion and rheological factors on formation of defect-free and ultrathin-skinned asymmetric polysulfone membranes for gas separation, Sep. Purif. Technol. 33 (2003) 127–143.

[23] A.K. Hołda, B. Aernouts, W. Saeys, I.F.J. Vankelecom, Study of polymer concentration and evaporation time as phase inversion parameters for polysulfone-based SRNF membranes, J. Memb. Sci. 442 (2013) 196–205.

[24] K. Hendrix, G. Koeckelberghs, I.F.J. Vankelecom, Study of phase inversion parameters for PEEK-based nanofiltration membranes, J. Memb. Sci. 452 (2014) 241–252.

[25] S. Cheng, D.L. Oatley, P.M. Williams, C.J. Wright, Positively charged nanofiltration membranes: review of current fabrication methods and introduction of a novel approach., Adv. Colloid Interface Sci. 164 (2011) 12–20.

[26] S. Cheng, D.L. Oatley, P.M. Williams, C.J. Wright, Characterisation and application of a novel positively charged nanofiltration membrane for the treatment of textile industry wastewaters., Water Res. 46 (2012) 33–42.

[27] D.L. Oatley-Radcliffe, S.R. Williams, C. Lee, P.M. Williams, Characterisation of Mass Transfer in Frontal Nanofiltration Equipment and Development of a Simple Correlation, J. Membr. Sep. Technol. 4 (2016) 149–160.

[28] S. Nicolas, B. Balannec, F. Beline, B. Bariou, Ultrafiltration and reverse osmosis of small non-charged molecules: a comparison study of rejection in a stirred and an unstirred batch cell, J. Memb. Sci. 164 (2000) 141–155.

[29] S.-I. Nakao, S. Kimura, Analysis of solutes rejection in ultrafiltration., J. Chem. Eng.

Japan. 14 (1981) 32–37.

[30] A.F. Ismail, A.R. Hassan, Formation and characterization of asymmetric nanofiltration membrane: Effect of shear rate and polymer concentration, J. Memb. Sci. 270 (2006) 57–72.

[31] N. Ali, N.S.A. Halim, A. Jusoh, A. Endut, The formation and characterisation of an asymmetric nanofiltration membrane for ammonia-nitrogen removal: effect of shear rate., Bioresour. Technol. 101 (2010) 1459–65.

[32] Hilal, N., A.F. Ismail, T. Matsuura and D.L. Oatley-Radcliffe, Membrane Characterization, Chapter 9, Elsevier, (2017), ISBN: 978-0-444-63776-5.

Figure and Table Captions

Figure 1: Chemical structure of polymers used, Top - PEI and Bottom - sPEEK.

Figure 2: Experimental filtration setup (1 – nitrogen gas bottle, 2 – pressure regulator, 3 – pressure indicator, 4 – Membranology HP350 stirred cell, 5 – magnetic stirrer plate, 6 – balance, 7 – computer data logger).

Figure 3: Performance of A6DTR membranes prepared by varying the polymer concentration in the casting solution.

Figure 4: SEM images of the membrane cross section for the prepared A6DTR polymer concentration experiments where: (a) 16 wt% (b) 19 wt% (c) 22 wt% (d) 25 wt% (e) 28 wt%.

Figure 5: SEM images of the membrane cross section for A6DTR polymer thickness experiment where: (a) 100 µm (b) 200 µm (c) 300 µm (d) 400 µm (e) 500 µm.

Figure 6: Performance of A6DTR membranes prepared by varying the wet thickness of the cast films.

Figure 7: Performance of the A6DTR membranes prepared with varying casting speed.

Figure 8: SEM images of membrane cross sections for A6DTR cast speed experiment where: (a) 100 µm (b) 200 µm (c) 300 µm (d) 400 µm (e) 500 µm.

Figure 9: Performance of A6DTR membranes prepared by varying the evaporation time.

Figure 10: SEM images of membrane cross sections for A6DTR evaporation time experiment where: (a) 10 s (b) 20 s (c) 30 s (d) 45 s (e) 60 s (f) 90 s.

Figure 11: Performance of A6DTR membranes prepared by varying the coagulation bath temperature.

Figure 12: SEM images of membrane cross sections for A6DTR coagulation bath temperature experiment where: (a) 3 °C (b) 10 °C (c) 20 °C (d) 30 °C (e) 40 °C (f) 50 °C.

Table 1: Composition of the experimental casting solutions and composition for polymer concentration experiment.

Figure 1

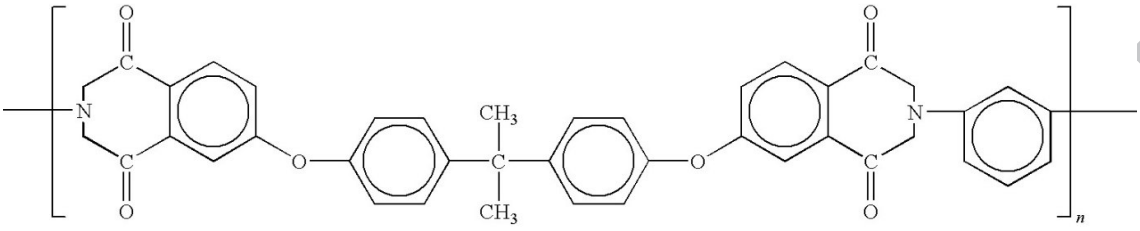

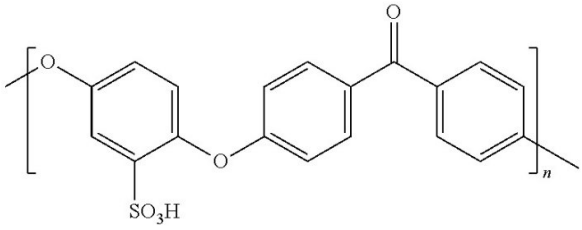

Figure 2

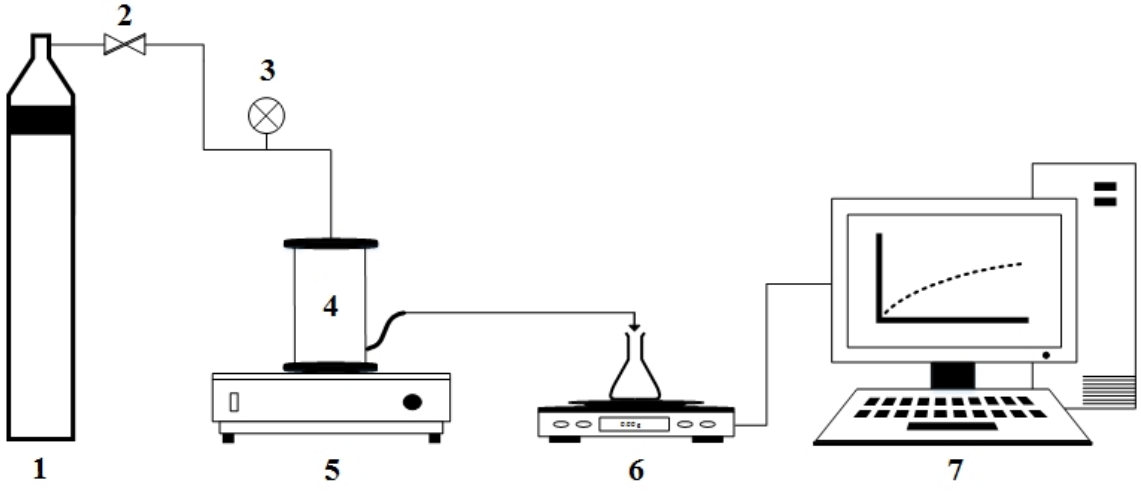

Figure 3

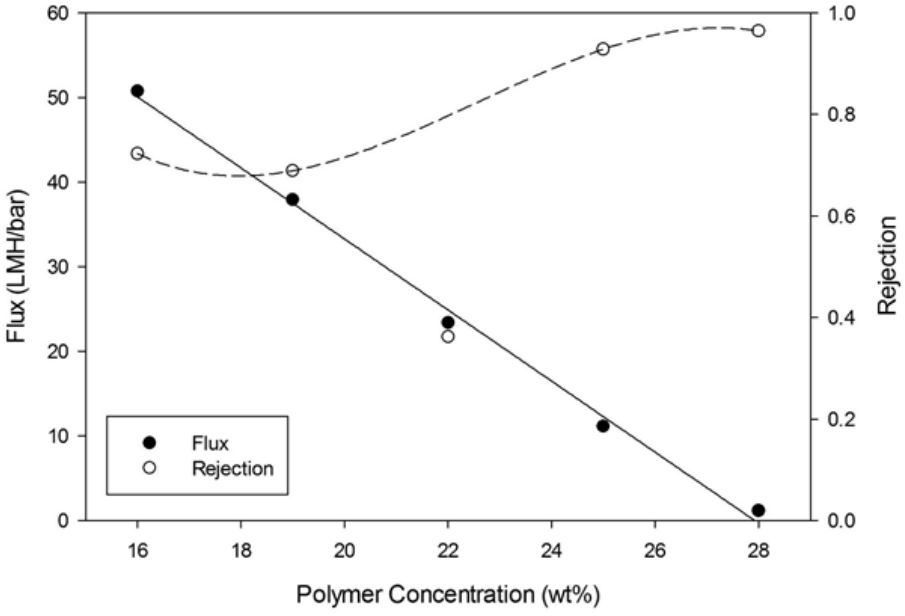

Figure 4

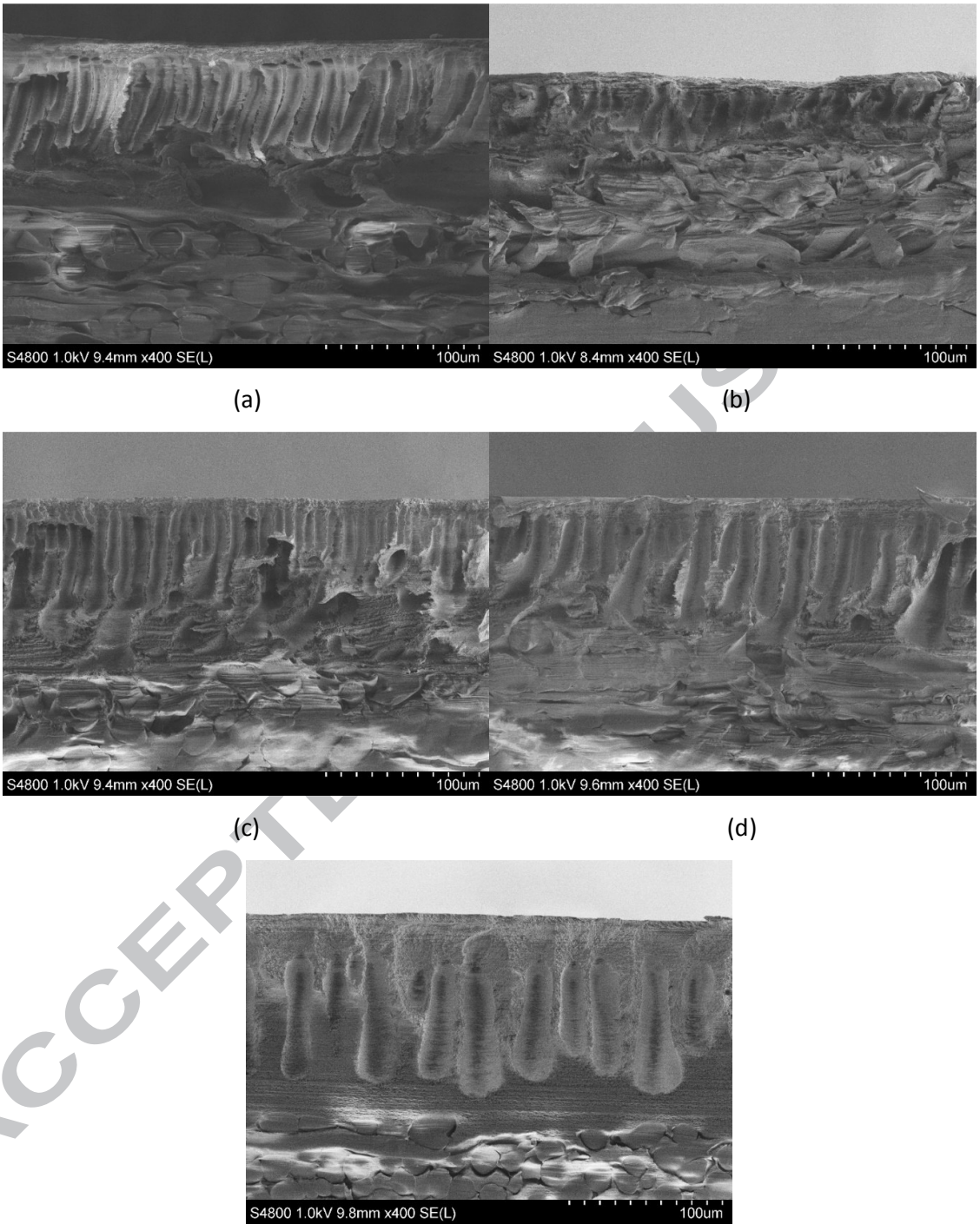

Figure 5

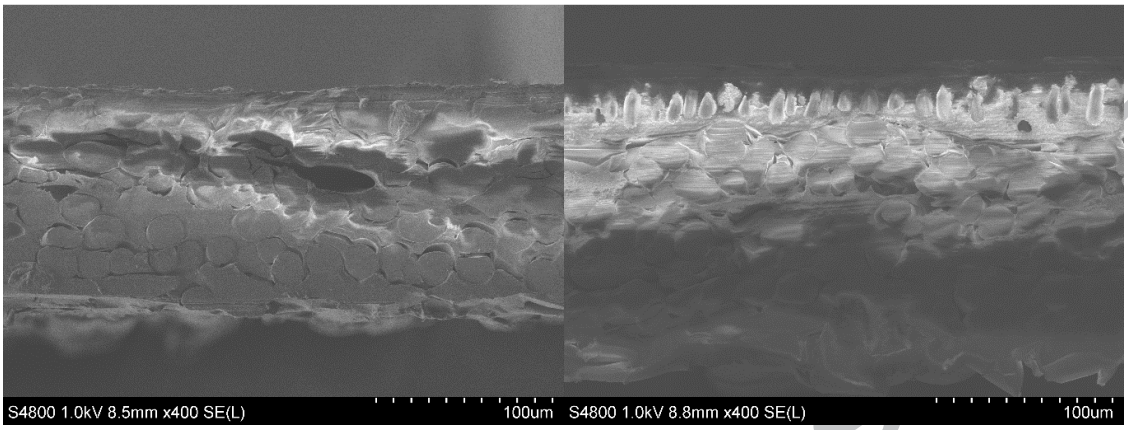

(a) (b)

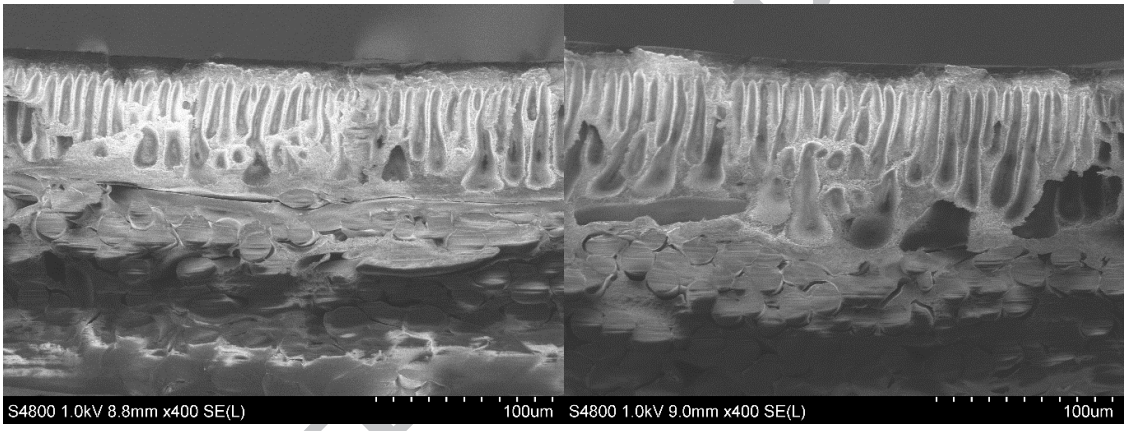

(c) (d)

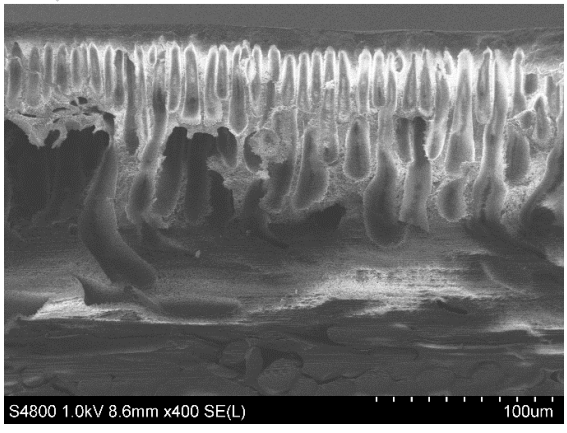

(e)

Figure 6

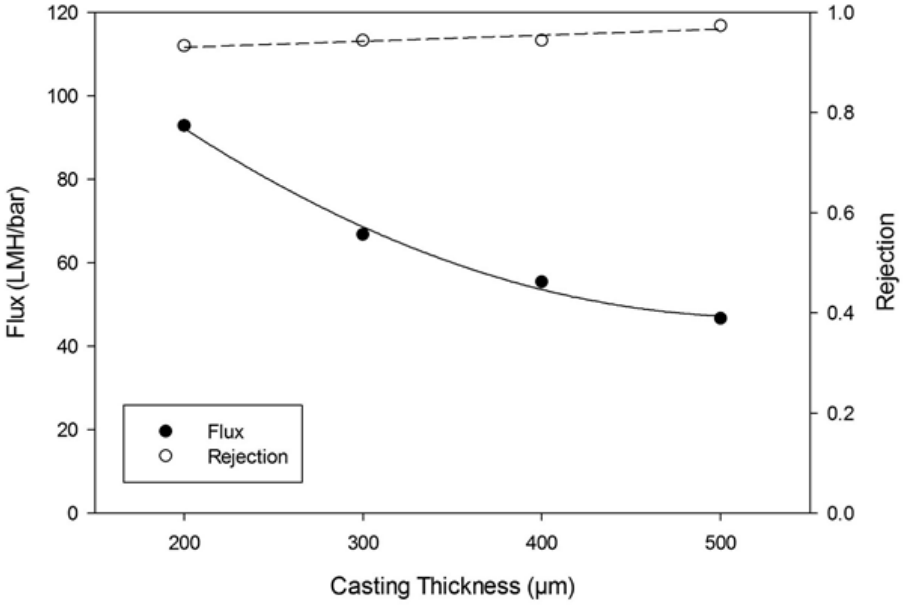

Figure 7

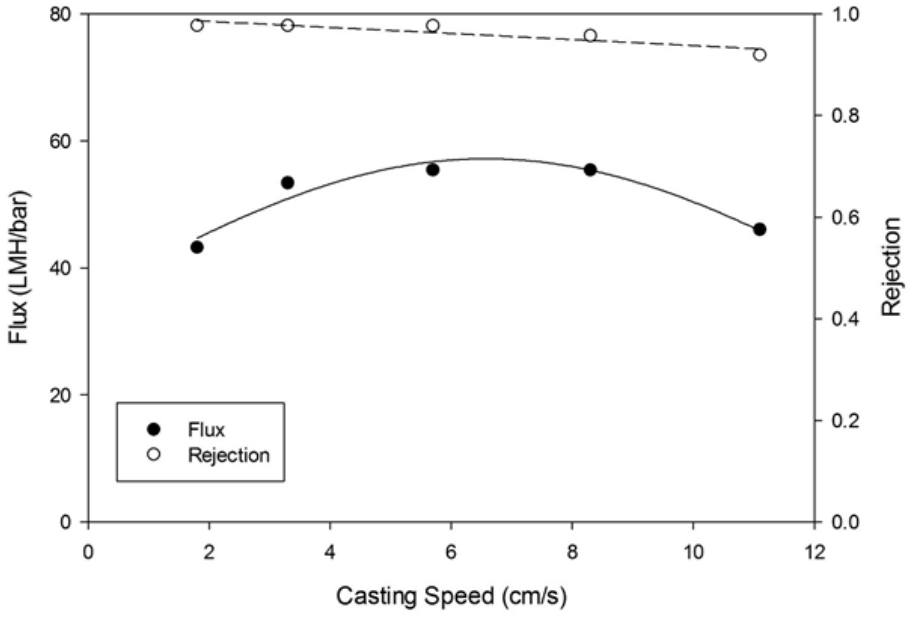

Figure 8

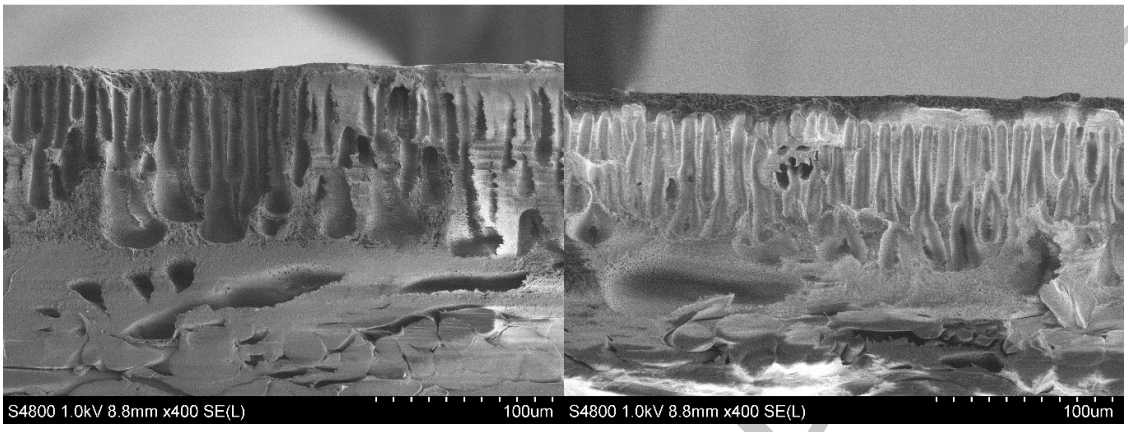

(a) (b)

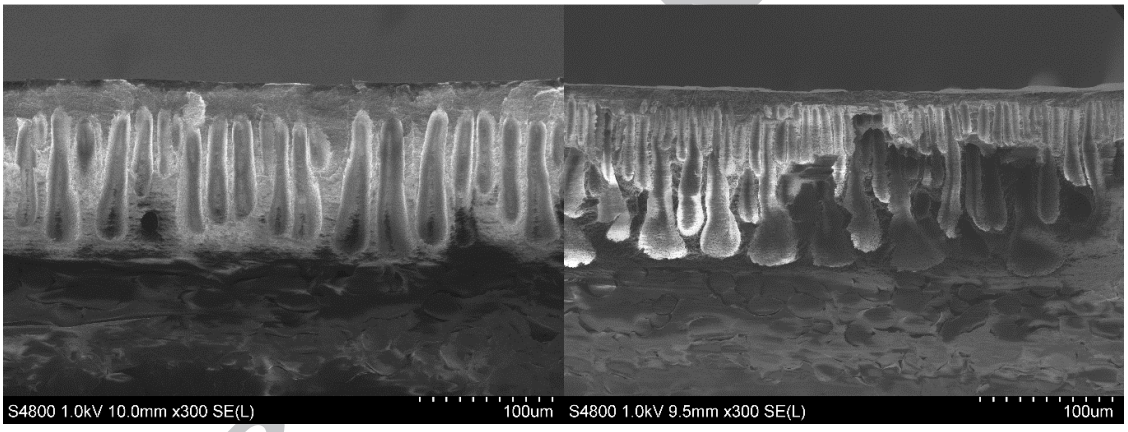

(c) (d)

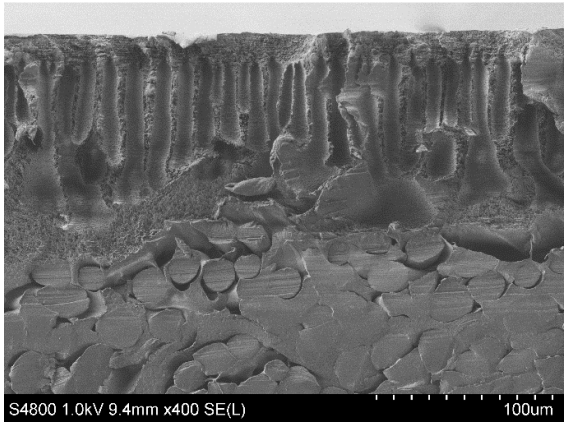

(e)

Figure 9

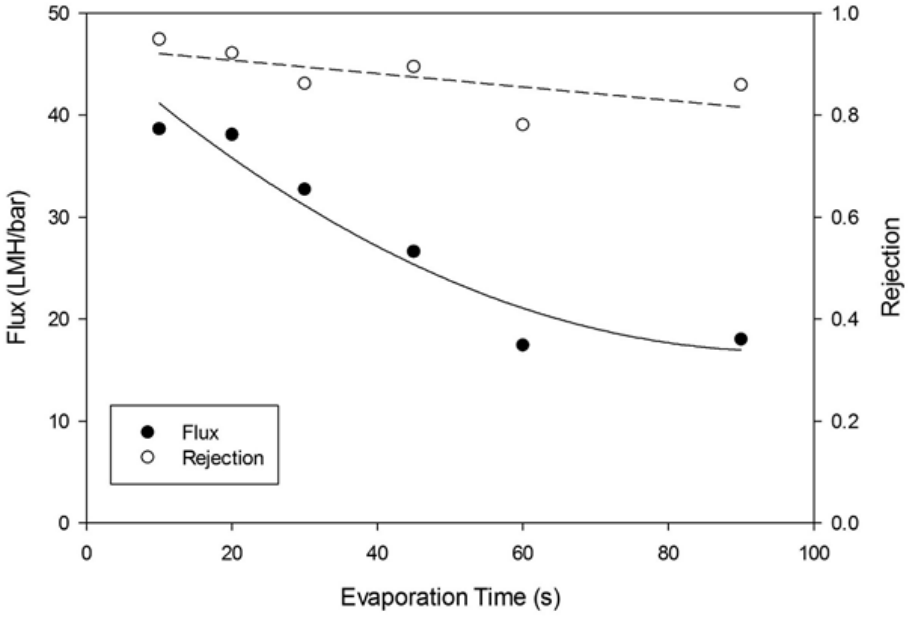

Figure 10

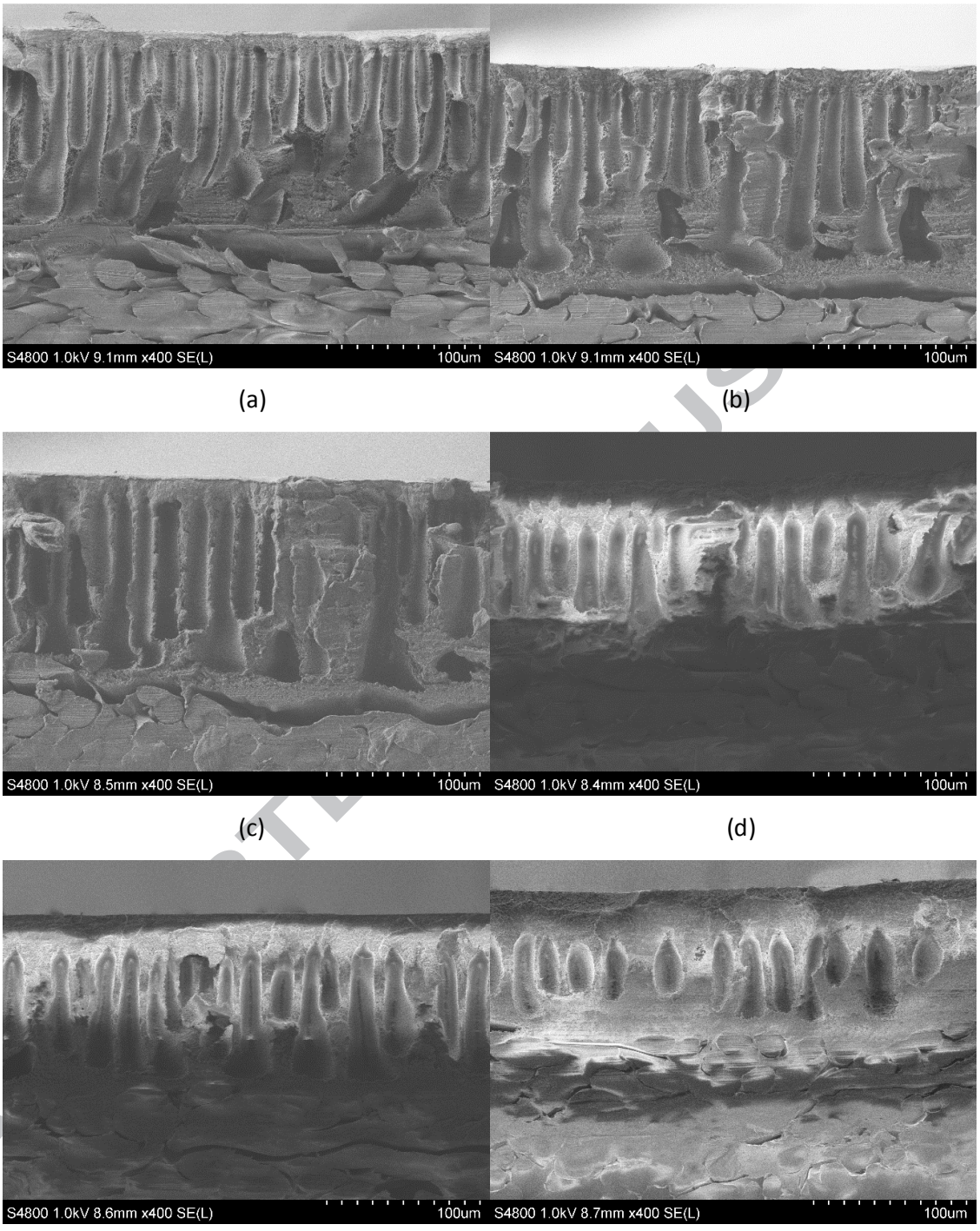

Figure 11

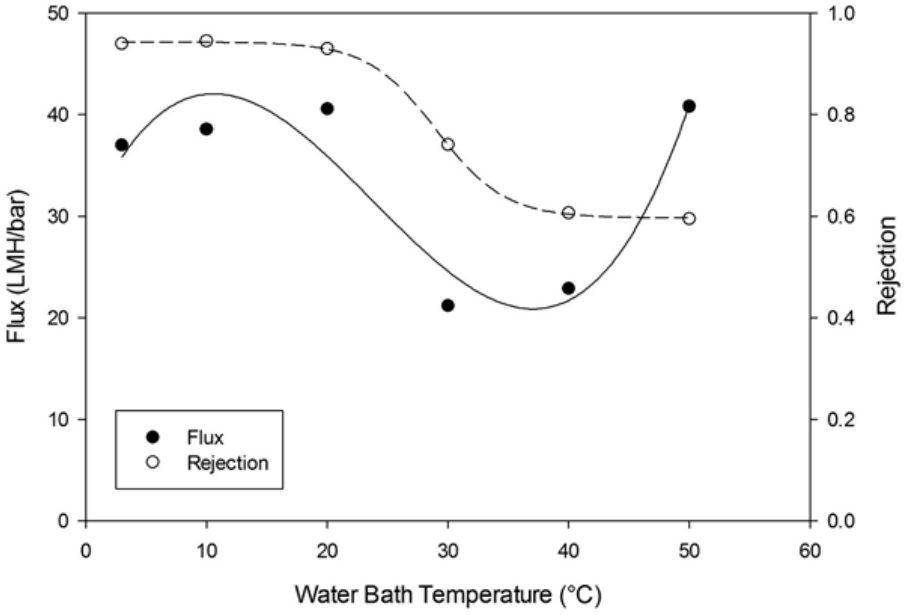

Figure 12

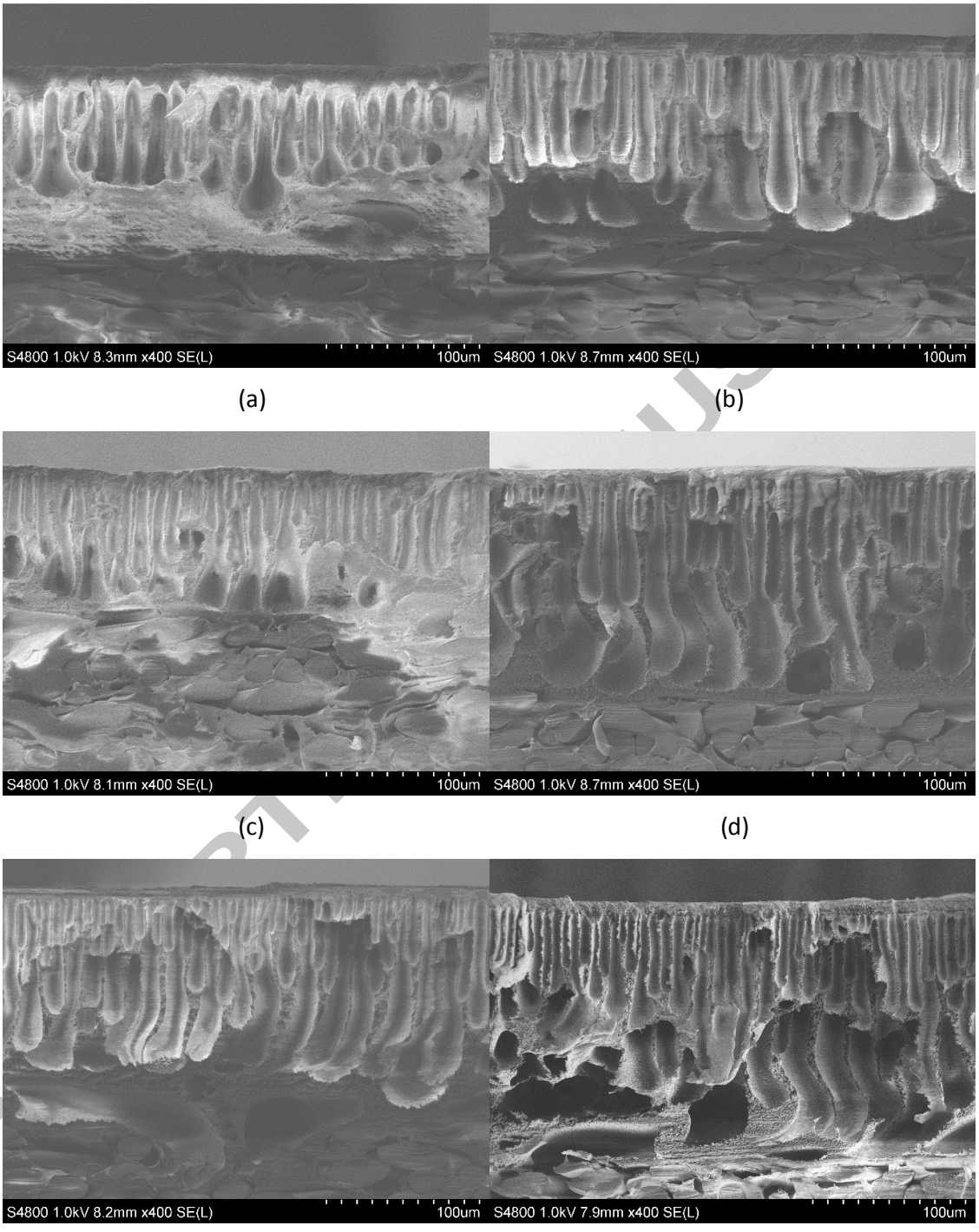

Table 1

	A6DTR	***Polymer Concentration Experiment***				
	~22 wt%	**16 wt%**	**19 wt%**	**22 wt%**	**25 wt%**	**28 wt%**
Composition (g)						
PEI	16	11.595	13.769	16	18.118	20.292
SPEEK	1	0.725	0.861	1	1.132	1.268
Total Polymer	*17*	*12.320*	*14.630*	*17*	*19.250*	*21.560*
Dioxane	1	1.078	1.040	1	0.963	0.924
THF	10	10.780	10.395	10	9.625	9.240
NMP	49	52.822	50.936	49	47.163	45.276
Total Solvent	*60*	*64.680*	*62.370*	60	57.750	55.440

Highlights

Phase inversion parameters are studied for a PEI-sPEEK blend membrane
Resultant membrane morphology is characterised by SEM
Membrane performance is characterised by flux and PEG rejection
Optimisation of these parameters produced controlled NF physical properties